LA-UR-17-22232
Approved for public release; distribution is unlimited.

Title: Review of X-ray Tomography and X-ray Fluorescence Spectroscopy

Author(s): Shear, Trevor A

Intended for: Report

Issued: 2017-03-16

3/13/2017

Review of X-ray Tomography and X-ray Fluorescence Spectroscopy

Shear, Trevor A
LOS ALAMOS NATIONAL LABORATORY

Abstract

This literature review will focus on both laboratory and synchrotron based X-ray tomography of materials and highlight the inner workings of these instruments. X-ray fluorescence spectroscopy will also be reviewed and applications of the tandem use of these techniques will be explored. The real world application of these techniques during the internship will also be discussed.

Introduction

Since the 1970's, X-ray tomography has been used to image and study the 3D structure of many materials and systems, ranging from plutonium in soil[1] to patient diagnosis[2,3]. The reason this technique is widely used is because of the nondestructive nature of the process, providing morphological detail from the micro- to nano- level without loss or damage to the system[4]. When analyzing material properties, this technique is extremely useful when applying a time component and studying the changes in the material in situ when it's exposed to a non-equilibrium situation[4]. Applying a compressive or tensile load, temperature changes, exposure to a corrosive environment, and/or applying an electrostatic force are widely used techniques to study material responses to these stimuli. Using these conditions on materials while imaging using X-ray tomography can give special insights in the response of a material, such as how polymeric foams buckle, how cracks propagate, and solidification in metals or polymers[5].

X-ray fluorescence (XRF) spectroscopy is another method using X-rays that can be used independently for elemental analysis of a material[6] or as a complimentary method to X-ray tomography[4,7]. While XRF is usually performed in only 2 dimensions, Los Alamos National Laboratory (LANL), has built a 3 dimensional XRF that can be used in conjunction with X-ray tomography to identify the 3D position of elements within a material.

Current State of the Art

The use of X-ray's to take an image through a material dates back to 1895, when German physicist Wilhelm Roentgen took the first radiograph. Since then, the use of radiographs has expanded from a primarily medical use, to use in industries from security screening to material science. Understanding the 3D morphology of materials and how they behave under various real world conditions in a non-destructive way is critical to understanding their short and long term performance[4,11].

Basic Principles of X-ray Tomography

The basic principles of X-ray tomography are fairly straight forward. X-rays are produced by a source. The X-rays pass through the sample which is rotating anywhere between 180 ^{o} and 360 ^{o} while radiographs are collected. The number of radiographs typically collected is more than 1000 and depending on the required exposure time of each radiograph, the collection of data can extend into multiple days[4]. Once the X-rays have passed through the sample, they impinge upon a scintillator, converted to visible photons and are focused by a lens to be finally recorded by a charge-coupled device (CCD) camera[4,8,9]. The collected images can then be processed by 3D imaging software such as Avizo® by FEI, efX-CT by North Star Imaging, DigiXCT by Digisens, Dragonfly by ORS, ImageJ, and ParaView.

X-ray Sources

There are four main sources of X-rays available; fixed anode, rotating anode, liquid metal jet, and synchrotron sources[4,8,9]. The former three are widely available while a synchrotron source is only available through a particle accelerator at national lab facilities. This discussion will focus on fixed, rotating, and synchrotron sources.

Fixed anode sources typically powered between one to 500W are the most common sources available. This is because they have fairly low maintenance, are quite robust, and come in a wide variety of anodes including Mo, Cr, Cu, Rh, and Ag[4]. With this source, however, the imaging resolution of the system is typically limited to approximately 5 micrometers[4].

Rotating anode sources can produce a 2.97 kW output and fluxes on the order of 10^9 photons/second[4]. Various types of anodes are available including, Cu, Cr, Mo, and Co. This type of source is capable of both nano- and micro-level resolutions. Because of their high brightness, these sources require much more maintenance than fixed anode sources. Depending upon usage, they are required to be rebuilt every few months[4]. With the appropriate X-ray optics, both the fixed and rotating sources are capable of reducing the chromaticity of the X-ray beam. This allows the instrument to isolate a specific element due to the beam energy, however, as the beam reduces chromaticity the flux through the sample is also reduced[9]. Generally, laboratory-based instrumentation does not produce enough flux to produce a useful monochromatic beam for imaging.

Synchrotron sources on the other hand are capable of producing a very bright beam[9]. Even though the X-ray energy is engineered to be brighter at low energy, the flux is extremely high, allowing the beam to become monochromatic but still be useable[4]. This source of X-rays is more specialized and harder to gain access to since they are generated at particle accelerators such as the Advanced Photon Source at Argonne National Laboratory[10], the Tevatron at Fermi National Accelerator Laboratory, and the Bevatron at Lawrence Berkley Laboratory. The increase in flux also allows for more radiographs to be taken in a smaller time frame, which can be crucial when an in situ experiment is being performed[4]. If the collection isn't fast enough, it's possible to miss a critical step in a failure analysis between radiographs. Generally, synchrotron sources are also equipped with the latest camera detectors, capable of frame rates from 0.01 to 1000 s^{-1} in comparison to lab-based camera frame rates of 0.01 to 0.1 s^{-1} [4,10].

Samples

Samples relating to material science such as superplastic forming[8], metallic foams[8], plastic foams[5], solidification of alloys[11], dentin[12], and biological samples (such as insects) can be imaged using X-ray tomography, but there are some limitations and potential barriers. One issue can arise when taking an image of a material with varying density[4,8,9]. More specifically, it's the electron density of the elements composed within the sample (generally electron density scales with atomic number and density of the material). For example, if the sample was a low density polymer foam with a gold interface, low energy X-rays would be able to image the foam but would be absorbed by the gold atoms and so you would only be able to image the foam[4]. Conversely, if you wanted to image the gold, you would need more energetic X-rays but these X-rays would simply pass through the foam without interacting and so you'd only be able

to image the gold[4]. This can cause the issue where you might not be able to image an entire material in one experiment, and you might not be able to image the entire material at all.

The size of the sample can be an issue as well. Depending on what is being imaged, you can be limited by the instrument being used. For example, an Xradia® microCT instrument using a fixed anode source is limited to an image size of approximately 1cm to 1mm wide field of view (FOV) with 3 – 30 µm resolution[4,13]. If a higher resolution is required, an Xradia® nanoCT with a rotating anode source can achieve 15 – 65 µm FOV with 50 – 150 nm resolution. Synchrotron FOV is from 1 cm to 4mm with up to 30 nm resolution[4,13,11]. The fixed anode source produces a diverging beam of X-rays which is capable of geometric magnification, unlike a synchrotron, which is a collimated beam and is not capable of this magnification[4].

X-ray Scintillators

Conversion of the X-ray's that pass through the sample to a form that can be detected by a CCD camera is done by use of a scintillator crystal. The scintillating material is usually one with a large band gap which is used to generate visible photons from the impact of the X-ray's[14]. The general process begins with an X-ray impacting the material, causing an electron to be excited from the valance band into the conduction band, which is completed in less than 1 ps[14]. Once the electrons in the conduction band have relaxed enough, they recombine with the hole in valance band and emit a visible photon (see Figure 1). Some materials (i.e., BaF_2) are also capable of electron transition from the valence band to the core band, causing another visible photon to be emitted[9,14]. Strong consideration is taken when making these materials because as flaws and defects occur, energy levels within the forbidden gap can form, causing performance degradation of the material[11].

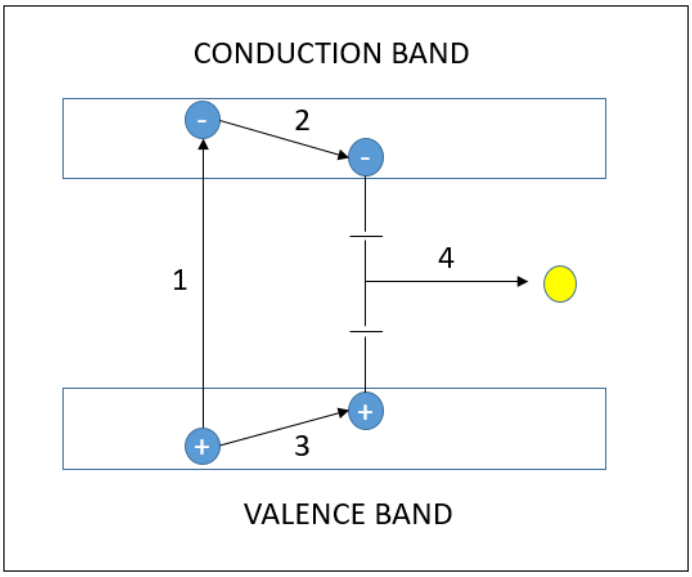

Figure 1: Diagram of a scintillator mechanism. 1) Excitation of an electron from the valence band to the conduction band. 2) Relaxation of the electron to the bottom of the conduction band. 3) Relaxation of hole to the top of the valence band. 4) Recombination of the electron-hole pair, resulting the emission of a photon.

X-ray Detectors

The detectors used in the systems discussed in this review is essentially a high quality CCD camera, meaning the sample moves while the source and detector stay stationary[9]. The scintillator absorbs the X-rays passing through the sample and converts the X-ray photons to visible light photons that can be detected by the CCD. The number of detector elements and the FOV of the camera dictates the resolution and how large (or small) of a sample can be used (although the flux of X-rays through the sample also play into this)[4,9]. The FOV and the number of detector elements also come into play when calculating the minimum voxel (volume element) by the relation: voxel = FOV/number of elements[9]. With increasing number of elements and deceasing FOV, the size of each voxel decreases.

The size of the total images collected can grow to be quite large depending on the type of detector used. For example, a detector with 1k x 1k elements, 16 bit images can be as large as 1 gigabyte[4]. Increase this to 2k x 2k at 16 bit and it increases up to 16 gigabytes per image[4,9]. The number of images taken during a normal CT can range between a few hundred to several thousand during the experiment and it's quite easy to have terabytes worth of data. This requires powerful workstations to compute this data and sophisticated reconstruction software.

Reconstruction Software

Most commercial instruments provide their own proprietary reconstruction software and a 3D rendering package. One such rendering application is Avizo ® by FEI. This package allows the upload of reconstructed images (such as .tiff files) collected by the instrument and renders them in 2D and 3D[4]. There are dozens of different types of filters and ways to look at the collected images. Figures 2-6 is a sample of what can be done using the software.

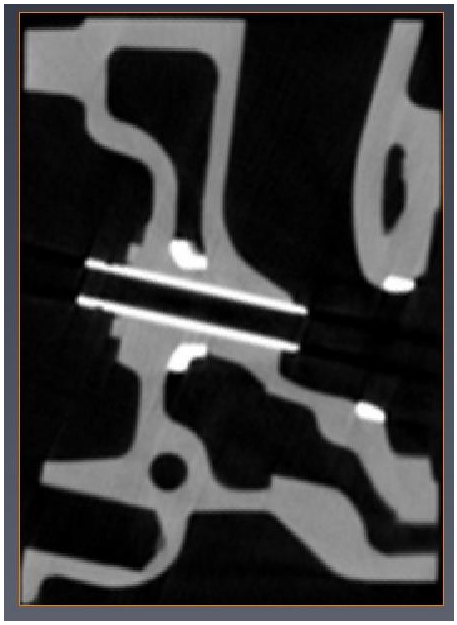

Figure 2: A single reconstructed slice of an X-ray CT of an engine. This is one picture of several hundred.

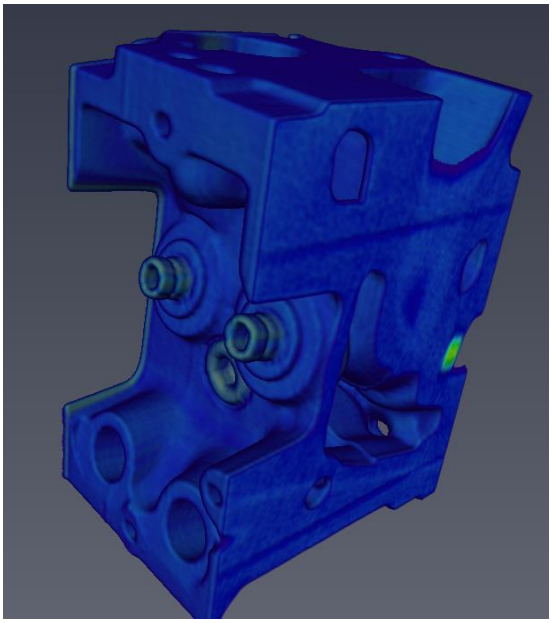

Figure 3: 3D rendering of all the reconstructed slices.

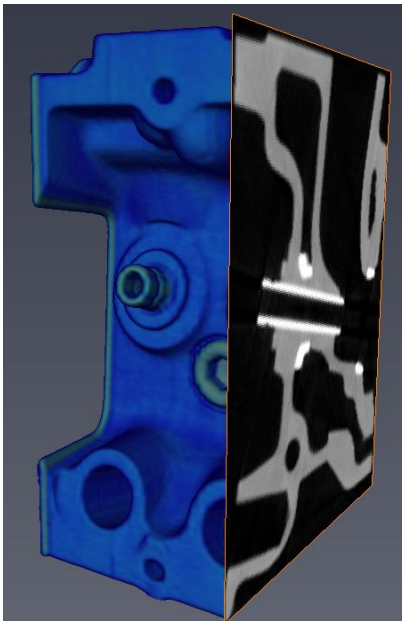

Figure 4: 3D rendering with a slice through it and the corresponding reconstructed slice at that location.

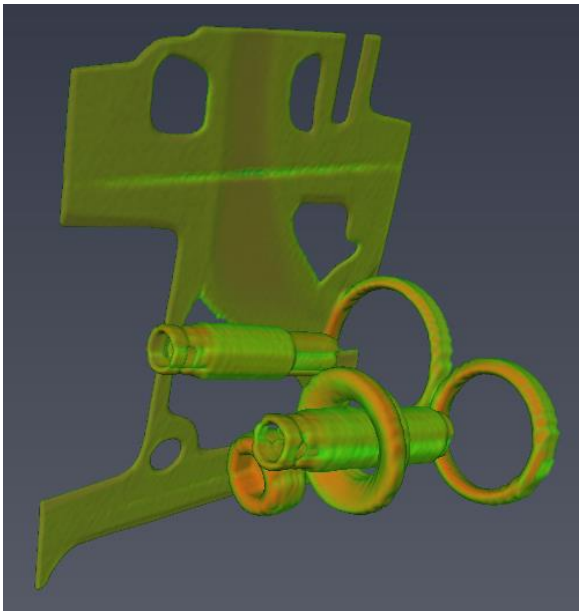

Figure 5: All the low density material has been removed by the software, showing only the high density components.

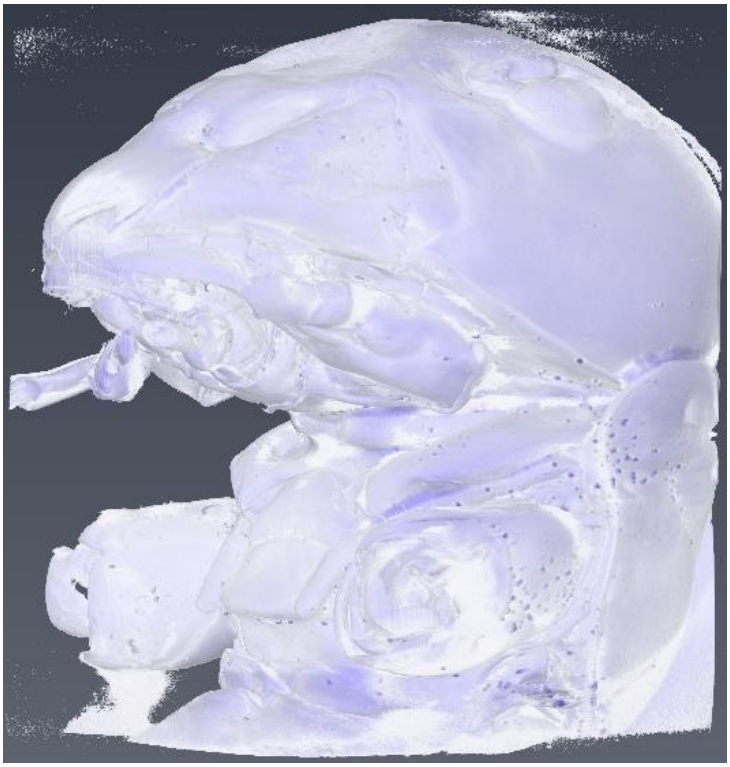

Figure 6: 3D rendering of Jerusalem Cricket (head only). Images collected at LANL using the Xradia® microCT.

The software not only reconstructs the images but also provides lots of useful data such as void(s) volume, void(s) size, material density, morphological properties, etc. Much of the filters used can also be automated through scripting languages such as Python or Tool Command Language (TCL) to make short work of large data sets.

X-ray tomography has advanced tremendously since the first radiograph was taken. X-ray sources have increased in power, detectors have become more sensitive and much faster, and computers are able to process the huge amount of data collected. These and other advances allow us to examine some of the most detailed properties of materials under real world conditions and fully explore their implications to cutting edge materials science challenges.

X-ray Fluorescence Spectroscopy

The basics of XRF (X-ray Fluorescence) are fairly simple. When a sample is irradiated with X-rays of sufficient energy, it ejects an inner orbital electron[4,6]. Electrons from higher orbitals then fall to fill the vacancy and as it goes to a lower energy state, it gives off a fluorescent X-ray which is analyzed[6] (see Figure 7). The energy of the fluorescent X-ray given off is characteristic of the energy difference between the two orbital energy levels and is specific to the element, while the intensity of the X-rays is related to the elements abundance in the sample[6].

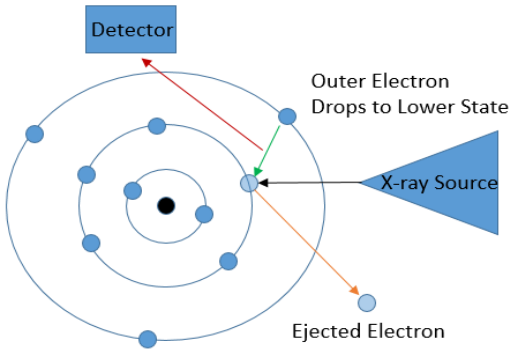

Figure 7: Diagram of how XRF produces fluorescence X-rays.

This technique is similar to X-ray photoelectron spectroscopy (XPS), except that XPS is detecting electrons ejected and their binding energy while XRF detects fluorescent X-rays emitted from an electron dropping to a lower energy state. While XPS is only able to detect elements around 10 nm into the surface of the material[15], with XRF it is possible to penetrate to several millimeters depending on the Z of the matix[4]. XRF is not able to detect the oxidation state or what other elements may be bound to the respective elements such as in XPS. Another function of XRF is that you can determine the density of a material[16]. The sensitivity of XRF is approximately in the percentage range[4].

One unique version of XRF available at LANL is a 3D XRF. While a standard 2D XRF setup uses one optic at the source for focusing, the 3D XRF uses a confocal setup where there is an optic for focusing at the detector as well[1,4,17]. The use of the confocal setup, in conjunction with a sample stage that moves in 3 dimensions, allows for 3D elemental profiling of the sample (see Figure 8). This can be very powerful because when you use this technique in tandem with X-ray CT imaging, it's possible to reconstruct a 3D image of the sample to show the morphology and the 3D elemental composition[1,17,18], whether it be at a laboratory setup or performed at a synchrotron.

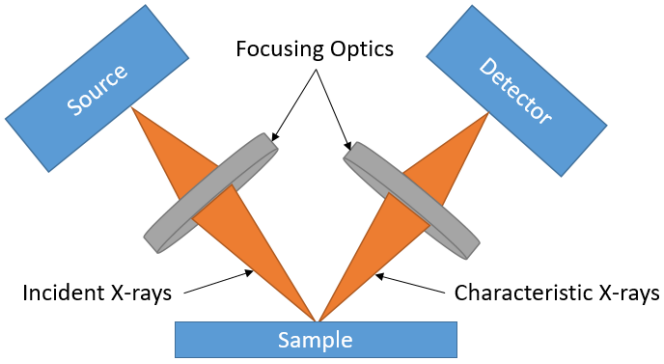

Figure 8: Diagram of a confocal setup for 3D XRF.

Future Directions

During my internship at LANL, I have been and will be exposed to quite a bit of X-ray tomography. At the lab, we have direct access to micoCT and nanoCT instruments that are used daily for several different projects. Currently I've been in the process of learning a programming language to reduce the time required to process data collected at the synchrotron. The resulting work from this project has taught me much about how to program and how it can be used to significantly speed up processing times of large data sets (multi terrabytes).

In April I will be traveling to Argonne National Laboratory to use the synchrotron at the Advanced Photon Source to collect real time data on various materials used in research and development. The materials tested will primarily be either compressed or have their tensile strength analyzed. The synchrotron is great for this because as you compress a material, if you aren't able to collect the images in near real time (such as with the microCT and nanoCT), the material can relax and data can be lost or skewed. With the speed at which the synchrotron can collect the images, this relaxation doesn't have time to occur and so the samples can be analyzed at a higher strain rate, producing results that align more closely to real world conditions.

While my training with X-ray tomography continues, I hope to start working with the XRF as well. However, the need for XRF is much lower than for the microCT and nanoCT, so it may be some time before I get to work more closely with that instrument. With all the instrumentation that's available for me to learn and work on here, I look forward to continuing to learn about X-ray tomography and XRF.

References

1. McIntosh, K. G.; Cordes, N. L.; Patterson, B. M.; Havrilla, G. J., Laboratory-based characterization of plutonium in soil particles using micro-XRF and 3D confocal XRF. *Journal of Analytical Atomic Spectrometry* **2015,** *30* (7), 1511-1517.
2. Chapman, D.; Thomlinson, W.; Johnston, R. E.; Washburn, D.; Pisano, E.; Gmür, N.; Zhong, Z.; Menk, R.; Arfelli, F.; Sayers, D., Diffraction enhanced x-ray imaging. *Physics in Medicine and Biology* **1997,** *42* (11), 2015.
3. Lewis, R. A., Medical phase contrast x-ray imaging: current status and future prospects. *Physics in Medicine and Biology* **2004,** *49* (16), 3573.
4. Patterson, B., Personal interview. Shear, T., Ed. 2017.
5. Patterson, B. M.; Cordes, N. L.; Henderson, K.; Williams, J. J.; Stannard, T.; Singh, S. S.; Ovejero, A. R.; Xiao, X.; Robinson, M.; Chawla, N., In situ X-ray synchrotron tomographic imaging during the compression of hyper-elastic polymeric materials. *Journal of Materials Science* **2016,** *51* (1), 171-187.
6. Potts, P. J.; Webb, P. C., X-ray fluorescence spectrometry. *Journal of Geochemical Exploration* **1992,** *44* (1), 251-296.
7. Cordes, N. L.; Seshadri, S.; Havrilla, G. J.; Yuan, X.; Feser, M.; Patterson, B. M., Three dimensional subsurface elemental identification of minerals using confocal micro-X-ray fluorescence and micro-X-ray computed tomography. *Spectrochimica Acta Part B: Atomic Spectroscopy 103–104*, 144-154.
8. Salvo, L.; Cloetens, P.; Maire, E.; Zabler, S.; Blandin, J. J.; Buffière, J. Y.; Ludwig, W.; Boller, E.; Bellet, D.; Josserond, C., X-ray micro-tomography an attractive characterisation technique in materials science. *Nuclear Instruments and Methods in Physics Research Section B: Beam Interactions with Materials and Atoms* **2003,** *200*, 273-286.
9. Stock, S. R., Recent advances in X-ray microtomography applied to materials. *International Materials Reviews* **2008,** *53* (3), 129-181.
10. Source, A. P. https://www1.aps.anl.gov/ (accessed March 7).
11. Salvo, L.; Suéry, M.; Marmottant, A.; Limodin, N.; Bernard, D., 3D imaging in material science: Application of X-ray tomography. *Comptes Rendus Physique* **2010,** *11* (9), 641-649.
12. Patterson, B. M.; Cordes, N. L.; Henderson, K.; Mertens, J. C. E.; Clarke, A. J.; Hornberger, B.; Merkle, A.; Etchin, S.; Tkachuk, A.; Leibowitz, M.; Trapp, D.; Qiu, W.; Zhang, B.; Bale, H.; Lu, X.; Hartwell, R.; Withers, P. J.; Bradley, R. S., In Situ Laboratory-Based Transmission X-Ray Microscopy and Tomography of Material Deformation at the Nanoscale. *Experimental Mechanics* **2016,** *56* (9), 1585-1597.
13. Hornberger, B.; Bale, H.; Merkle, A.; Feser, M.; Harris, W.; Etchin, S.; Leibowitz, M.; Qiu, W.; Tkachuk, A.; Gu, A.; Bradley, R. S.; Lu, X.; Withers, P. J.; Clarke, A.; Henderson, K.; Cordes, N.; Patterson, B. M. In *X-ray microscopy for in situ characterization of 3D nanostructural evolution in the laboratory*, 2015; pp 95920Q-95920Q-11.
14. Martin, N., Scintillation detectors for x-rays. *Measurement Science and Technology* **2006,** *17* (4), R37.
15. Seah, M. P., A review of the analysis of surfaces and thin films by AES and XPS. *Vacuum* **1984,** *34* (3), 463-478.
16. Patterson, B. M.; Campbell, J.; Havrilla, G. J., Integrating 3D images using laboratory-based micro X-ray computed tomography and confocal X-ray fluorescence techniques. *X-Ray Spectrometry* **2010,** *39* (3), 184-190.
17. Lühl, L.; Mantouvalou, I.; Schaumann, I.; Vogt, C.; Kanngießer, B., Three-Dimensional Chemical Mapping with a Confocal XRF Setup. *Analytical Chemistry* **2013,** *85* (7), 3682-3689.
18. Woll, A. R.; Mass, J.; Bisulca, C.; Huang, R.; Bilderback, D. H.; Gruner, S.; Gao, N., Development of confocal X-ray fluorescence (XRF) microscopy at the Cornell high energy synchrotron source. *Applied Physics A* **2006,** *83* (2), 235-238.